

Biodegradable Superabsorbent Hydrogel from Activated Hydrochar-Glycerol Cross-linked with Maleic Acid

Stanley M. Mukulu¹, Harun M. Mbuvi¹, Titus M. Kasimu², Francis Maingi^{3,*}

¹Department of Chemistry, Kenyatta University Nairobi, Kenya

²Department of Physical Sciences, Machakos University, Kenya

³Department of Science Technology and Engineering, Kibabii University, Kenya

Abstract Superabsorbent hydrogels are polymer materials with a three-dimensional structure. They have the potential to absorb large amounts of water or aqueous solutions due to the presence of hydrophilic functional groups in their network structures. The increasing population, coupled with advanced technologies, has led to a fourfold increase in demand in industrial applications, technological fields, medical fields, and agriculture. This study reports on the synthesis and characterization of superabsorbent hydrogels derived from activated hydrochar. The preparation of hydrochar was done via the dehydration process of sugarcane bagasse, followed by activation using acidified potassium permanganate to form activated hydrochar (AH). The AH was then reacted with glycerol to form polymer units (AHGL). The polymeric units were then reacted with maleic acid to form a superabsorbent hydrogel (SAH). Characterization of the synthesized SAH was carried out using FT-IR, SEM, and XRD. The swelling capacity was optimized by varying contact time and doses of both glycerol and maleic acid. The FT-IR spectra showed a C=O carbonyl spectral absorption peak at 1711.85 cm^{-1} in SAH, indicating successful crosslinking. The XRD analysis portrayed the amorphous nature of hydrochar and AH, while AHGL and SAH showed semi-crystalline and crystalline nature, respectively. SEM analysis showed dense porous surfaces in SAH compared to rigid surfaces with fewer and unevenly distributed pores in AHGL. The gravimetric technique showed that the maximum absorption capacity of the SAH was obtained at the optimum reaction mole ratio of AH:GL:MA of 10:4:1. The maximum absorption capacity of the synthesized superabsorbent hydrogel relative to its dry mass was found to be 905% and was achieved in a period of 8 hours. Crosslinking the hydrogel improved the water absorption capacity, and hence, it has potential application in agriculture in arid and semi-arid regions.

Keywords Absorption, Activated hydrochar, Superabsorbent, Cross-linker and Glycerol

1. Introduction

Superabsorbent hydrogels refer to crosslinked three-dimensional polymeric network structures with hydrophilic functional groups. Some of these hydrophilic groups include $-\text{SO}_3\text{H}$, $-\text{OH}$, COOH , and NH_2 groups [1]. These groups enable the compounds to absorb and retain a considerable amount of water through the formation of hydrogen bonds, with some absorbing as much as 500-1500 g/g [2]. The ability to absorb and retain water makes these hydrogels highly applicable in various fields, including industrial, agricultural, healthcare, and technological applications. Hydrogels can be categorized as chemical or physical hydrogels and are synthesized based on their crosslinking mechanism (physical and chemical crosslinking mechanisms) [3]. Chemically

crosslinked hydrogels are prepared through addition and condensation polymerization, chain growth polymerization, and electron and gamma radiation polymerization techniques. Physically crosslinked hydrogels are synthesized by crystallization, hydrophobized polysaccharides, ionic interaction, stereo complex formation, and hydrogen bond techniques [4]. The addition of the cross-linkers between the polymer chains affects hydrogels' properties, such as mechanical strength, swelling, solubility, and elasticity [5]. Many of the existing synthetic hydrogels are non-biodegradable, or their rate of degradation is very slow, leading to the accumulation of polymer materials in the soil, which causes environmental pollution [6], [7]. Therefore, this becomes a driving motive for researchers to develop superabsorbent hydrogels that are biodegradable. This study aimed at preparing biodegradable and high-performance superabsorbent hydrogels from sugarcane bagasse (biomass), which is a waste with high cellulose content, and then evaluating their absorption behaviour.

* Corresponding author:

mukoramaingi@gmail.com (Francis Maingi)

Received: Jul. 22, 2025; Accepted: Aug. 10, 2025; Published: Aug. 13, 2025

Published online at <http://journal.sapub.org/ajps>

2. Materials and Methods

2.1. Chemical and Reagents

Sugarcane bagasse was obtained from Kiambu County, Kenya and transported to Kenyatta University laboratories. Glycerol (1.261 g/cm³), maleic acid, sodium hydroxide, acidified potassium permanganate and concentrated sulphuric acid were obtained from Kenya Chemical Company, and they were pure and utilized as received.

2.2. Preparation of the Hydrochar

Hydrochar was prepared using the procedure adopted from Isahak [8] with slight modifications. Clean and dry pieces of sugarcane bagasse were fully immersed in 100 mL of 18 M concentrated sulphuric acid in a 1000 mL glass beaker for 30 minutes to ensure complete dehydration at room temperature. Filtration was done, and the residue obtained was washed with excess deionized water to remove excess acid and then dried in an oven at 80°C to a constant weight.

2.3. Preparation of Activated Hydrochar (AH)

The preparation of activated hydrochar was done using a procedure adopted from Yahya [9] with slight modifications. Dry hydrochar was crushed and ground using an agate pestle and mortar to obtain fine powder. A sample of 20 g of fine hydrochar was immersed in 600 mL of 2 M acidified potassium permanganate in a 1000 mL glass beaker for 16 hours to ensure that the hydrochar was fully oxidized. The mixture was then filtered using Whatman no. 42 filter paper. The residue obtained was washed with excess deionised water until all of the purple colour of potassium permanganate was removed. It was then dried in an oven at 80°C to a constant weight. The activated hydrochar sample was coded as (AH). The oxidation reaction introduces oxygen functional groups on the surface of the hydrochar that was used to link with glycerol through the esterification process to form polymer units.

2.4. Synthesis of Activated Hydrochar Glycerol Units AHGL

The procedure for the synthesis of the polymer units (AHGL) was adopted from Titus *et al.* [10] with some modifications. The dry activated hydrochar obtained was crushed and ground using an agate pestle and mortar to form fine powder. 20 g of AH was accurately weighed using a CZ-200 electric weighing balance and placed in a 250 mL round-bottomed flask. About 30 mL of deionized water was added to the flask while stirring to form a black suspension. The mixture was then refluxed using an electric heater for 10 minutes. About 8 mL of glycerol was added to the boiling AH suspension, followed by the addition of 10 mL of 2 M sodium hydroxide solution (catalyst). The mixture was then refluxed for 3 hours, after which it was dried in an oven at 100°C until a constant mass of activated hydrochar glycerol polymer units coded as (AHGL) was obtained.

2.5. Synthesis of Functionalized AHGL Cross-Linked with Maleic Acid (SAH)

SAH was prepared from AHGL as described in section 2.4. After the addition of sodium hydroxide and refluxing for three hours, 10 mL of 0.1 M maleic acid solution was added to the boiling solution of AHGL. Refluxing was continued for another 2 hours. The refluxed mixture was then placed in an oven to dry at 80°C, followed by cooling in a desiccator to obtain a superabsorbent hydrogel that was coded as SAH.

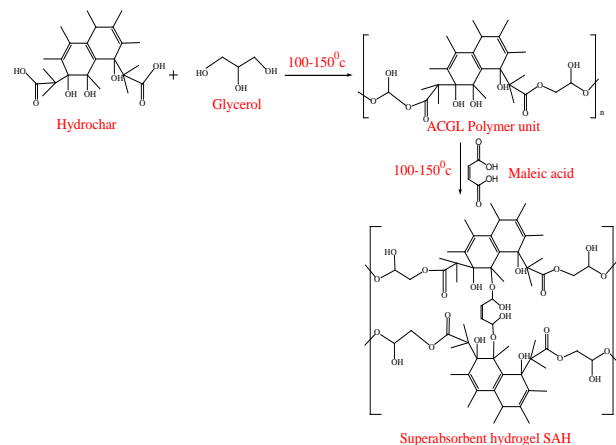


Figure 1. Schematic diagram for preparation of AHGL and SAH

2.6. The Swelling Capacity of SAH

The absorption percentage capacity of the superabsorbent hydrogel (SAH) samples was determined gravimetrically using the tea bag method [11]. The samples of 2.0 g were placed in the permeable polyester bags, and the total mass was recorded as (Y). The tea bags were then immersed in 600 mL of deionized water in a 1000 mL beaker. After 24 hours, they were removed, and the water adhering to the surface of the polyester bags was wiped using tissue paper. They were then weighed, and their mass was recorded as (X). The percentage absorption capacity of the hydrogel samples was calculated using equation 1 [12].

$$\% \text{ Swelling capacity} = \left(\frac{Y-X}{X} \right) \times 100 \quad (1)$$

Where Y is the weight of the swollen hydrogel samples
X is the weight of the dry hydrogel samples.

2.7. Effect of Glycerol Dosage on Swelling Capacity of Cross-Linked Hydrogel (SAH)

The effect of glycerol was studied by synthesizing 5 samples of SAH in triplicate by varying the volumes of GL in the range of 2, 4, 6, 8, and 10 mL. Activated hydrochar, maleic, and NaOH were maintained at 10 g, 5 mL of 2.0 M, and 5 mL of 2 M, respectively. 2 g of the prepared hydrogel samples were accurately weighed and then immersed in distilled water, in triplicate, for 24 hours, followed by determination of the mean percentage swelling.

2.8. Effect of Maleic Dosage on Swelling Capacity of Cross-Linked Hydrogel (SAH)

The effect of the dose of the MA (cross-linker) was determined by preparing 5 samples of SAH in triplicate at varied concentrations of 1, 2, 3, 4, and 5 M while maintaining the doses of AH, GL, and NaOH at 10 g, 4 mL, and 5 mL of 2 M, respectively. Accurately weighed 2 g of the synthesized hydrogel samples were immersed in distilled water in triplicate for 24 hours, followed by the determination of the mean percentage swelling.

2.9. Effect of Contact Time on Swelling Capacity of Cross-Linked Hydrogel (SAH)

The effect of the contact time of the superabsorbent hydrogel synthesized at optimum ratio conditions was determined by immersing 2 g of 24 accurately weighed portions of SAH in distilled water. The samples were then removed in triplicate at every designated time interval of 0.5, 1, 2, 4, 6, 8, 12, and 24 hours from water and weighed to determine the mean percentage swelling capacity.

2.10. Characterization of Hydrogels

2.10.1. Fourier Transform Infrared (FTIR)

Functional groups of the hydrochar, AH, AHGL, and SAH, were determined using FT-IR (Shimadzu IR Tracer-100) according to the procedure described by Kulkarni [13]. The prepared samples were then dried in an oven until a constant mass was achieved. They were then ground using a mortar and agate pestle to obtain fine powder. The dry samples of each hydrochar, AH, AHGL, and SAH, were mixed with pre-dried KBr in a ratio of 25:1 mg, respectively. The fine homogenous mixture was compressed to form a transparent pellet, then analyzed using the FT-IR at a wavelength between 400 and 4000 cm^{-1} .

2.10.2. Scanning Electron Microscope (SEM)

The SEM analysis for the prepared samples of hydrochar, AH, AHGL, and SAH was carried out to examine the microscopic structure and the surface morphology. The analysis was done using a Scanning Electron Microscope TESCAN VEGA (SEM) operating at an accelerating voltage of 20 kV. The samples were dried in an oven to a constant mass, followed by crushing and grinding using a mortar and agate pestle to obtain powdered samples. The fine samples were gold-coated to reduce electric charging, mounted on carbon tape, then enclosed in glass, ready for analysis to obtain micrographs [14].

2.10.3. X-ray Diffraction (XRD)

The phase composition of the hydrochar, AH, AHGL and SAH samples was determined using a Philips X'Pert instrument at 40 mA with $\text{CuK}\alpha$ radiation at 0.1541 nm. A monochromatic beam with a step size of 0.0170 (2θ), a time step of 175.26 s, and a scan range of 2θ from 0 to 100° was applied. The samples were dried in an oven to a constant

weight, crushed and ground using a mortar and pestle to a fine powder. The powdered samples were mounted flat on slides and then placed in the XRD instrument to obtain diffractogram [15].

3. Result and Discussions

3.1. Fourier Transform Infrared Spectroscopy for Hydrochar, AH, AHGL and SAH

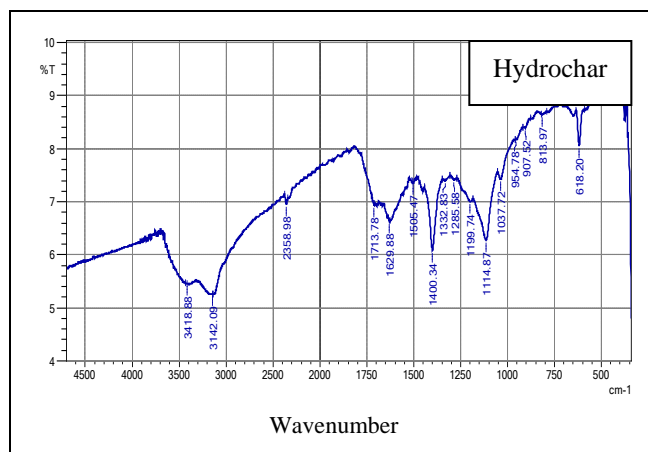


Figure 2A. FT-IR Spectrum of hydrochar

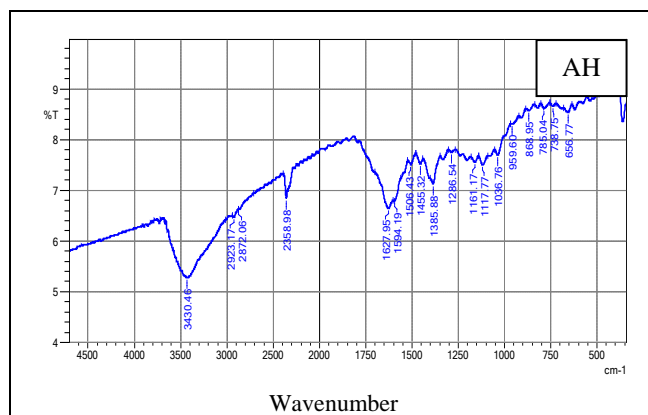


Figure 2B. FT-IR Spectrum of AH

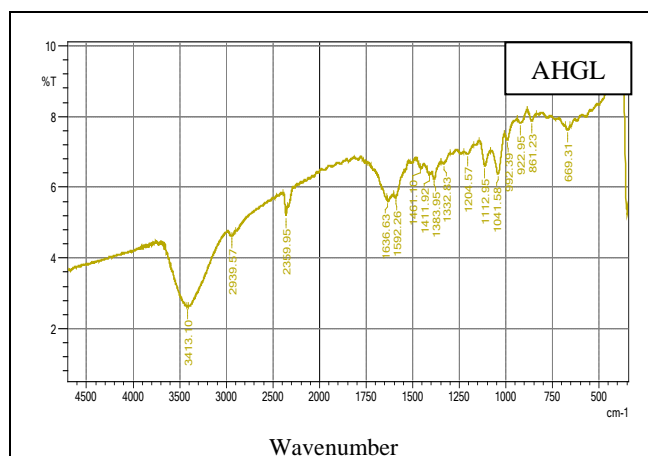


Figure 2C. FT-IR Spectrum of AHGL

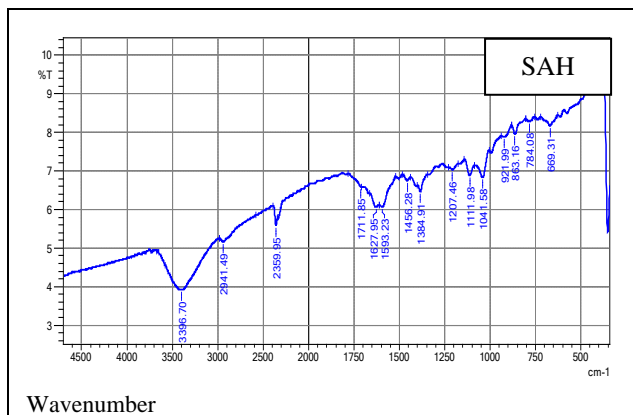


Figure 2D. FT-IR Spectrum of SAH

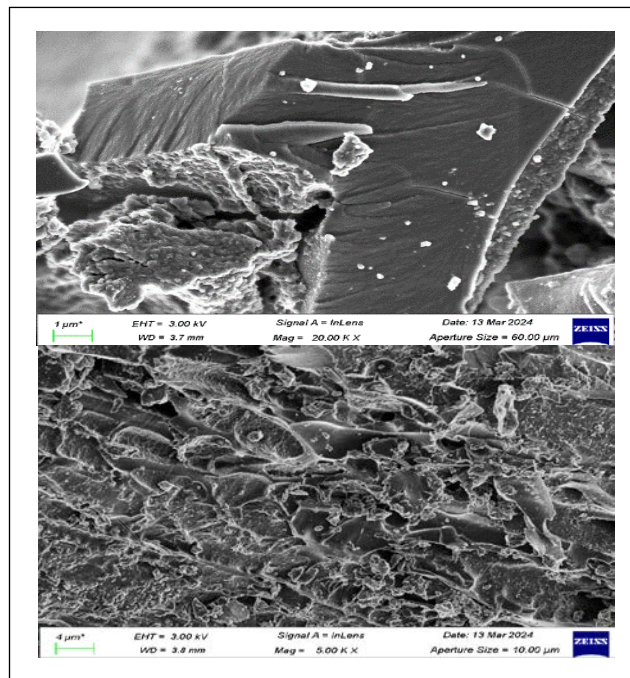
The FT-IR analysis was used to evaluate the functional groups present on the prepared samples of hydrochar, AH, AHGL, and SAH. Figures 2A, 2B, 2C, and 2D show the IR spectra of the sugarcane bagasse hydrochar, AH, AHGL, and SAH, respectively.

The hydrochar spectrum Figure 2A showed a broad spectral band at 3418.88 cm^{-1} and 3142.09 cm^{-1} was attributed to -OH for alcoholic and phenolic groups [16]. The peak at 1713.78 cm^{-1} represents the stretching vibration of the C=O carbonyl group for aldehyde [17]. The intense bands at 1629.88 cm^{-1} correspond to skeletal vibration stretching for the C=C aromatic ring [18]. The sharp, intense band at 1400.34 cm^{-1} represents C-H bending stretch [19]. The sharp peaks at 1114.87 cm^{-1} and 1037.72 cm^{-1} corresponded to C-O for the alcoholic, ether and phenolic groups while the 954.78 cm^{-1} absorption peak belonged to -OH out of plane bending for the alcoholic and phenolic groups [20]. Figure 2B for AH was obtained upon activation of the hydrochar and showed a new spectral peak at 1594.19 cm^{-1} attributed to the C=O carbonyl stretch vibration for the carboxylic acid, indicating successful oxidation on the surface of the hydrochar [21].

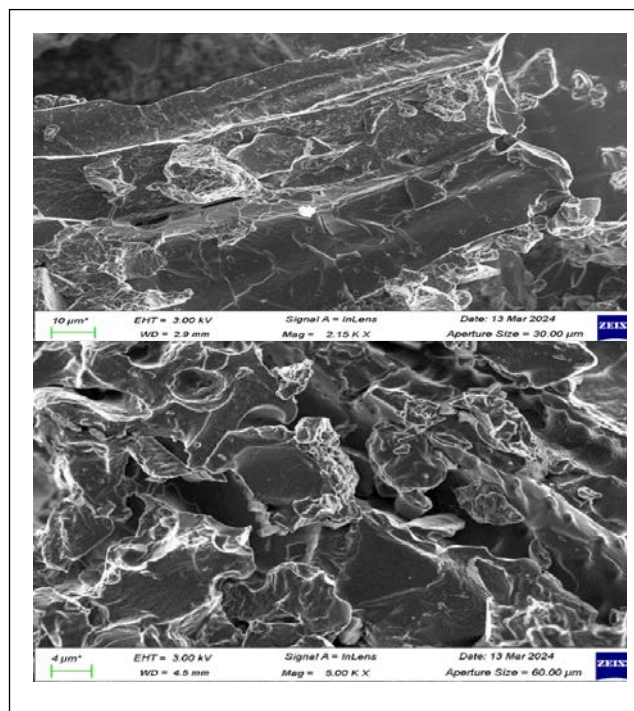
Upon functionalization of AH with GL, figure 2C for (AHGL) was obtained, showing a wide broad peak at 1636.63 cm^{-1} attributed to COO^- stretching vibration of an ester [22]. This peak indicated that the ester-linkage between the carboxyl functional groups of AH and the hydroxyl functional groups of glycerol (GL) was successful. However, figure 2D for SAH showed a new peak at 1711.85 cm^{-1} ascribed to COO^- group of an ester as compared to peaks in figure 2C. This peak showed clearly that there was a successful ester cross-linkage reaction between polymer units of AHGL and MA to form superabsorbent hydrogel SAH [23].

3.2. Scanning Electron Microscope Analysis for Hydrochar and AH, AHGL and SAH

Microstructure analysis of the hydrochar, AH, AHGL and SAH was done using scanning electron microscope (SEM). The Figure 3 below shows the surface morphology of the prepared hydrochar, AH, AHGL and SAH.



Figures 3A. SEM Micrograph of hydrochar and AH, respectively



Figures 3B. SEM Micrograph of AHGL and SAH, respectively

The micrograph for the hydrochar (Figure 3A) showed smooth layered structures that had flat surfaces with cracks and a small number of pores (white particles). This shows that during the dehydration process, the volatiles were removed, consequently creating a large surface area of the hydrochar [24]. The large surface area was the target for the excellent introduction of carboxylic groups during the oxidation process. Upon activation of the hydrochar,

the external surface of the AH (Figure 3A) developed a quasi-cleavage like fractured surface with rough, larger cavities, wider pore network, crevices, and crater-like surfaces that indicated a higher surface area [25]. This was due to the introduction of oxygen on carbon chains of hydrochar forming carboxylic and carbonyl groups. These groups were required for the reaction between the activated hydrochar monomer and the GL co-monomer forming polymer units. The AHGL micrograph (Figure 3B) was obtained after functionalization of AH with GL and showed a quasi-fractured like crystalline surface that was intact and rigid with cracks and fewer voids [14]. Upon crosslinking the polymer units of AHGL hydrogel with MA, a large, uniformly distributed porous surface network of SAH (Figure 3B) was obtained.

3.3. X-ray Diffraction Analysis of the Hydrochar AH, AHGL and SAH

The XRD technique was employed to determine the degree of crystallinity of the hydrochar, AH, AHGL and SAH as shown in Figure 4.

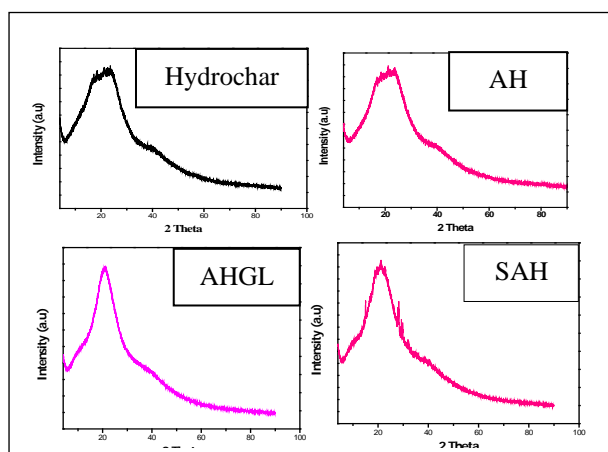


Figure 4. XRD Diffractogram of hydrochar, AH, AHGL and SAH

The diffractogram figure 4 at the 2θ angle range showed that the hydrochar had a single diffused broad peak with an intense peak at 250, indicating that it was amorphous. On activation, a broad hump with an intense peak at 250 confirmed the amorphous structure of hydrochar and AH [26]. This indicated that lignin and hemicellulose were present, as they are both amorphous, and that the crystalline cellulose chains were partially destroyed during the dehydration process of the sugarcane bagasse [27]. The diffractogram of AHGL and SAH showed sharper and higher peaks in the 2θ angle range at 200, indicating a semi-crystalline form for polymer units AHGL and superabsorbent hydrogel SAH compared to hydrochar and AH. The semi-crystalline phases were attributed to the presence of carboxylate groups formed during polymerization and crosslinking processes [28]. On the other hand, the diffractogram of SAH showed an increased number of sharp peaks in the 2θ angle range at 190 and 280 as compared to the AHGL diffractogram. This showed a change of morphology from semi-crystalline in

AHGL to crystalline in SAH. The cross-linker increased the number of hydroxyl groups, leading to a high rate of hydrogen bond formation responsible for supporting the stability of the crystalline phase structure of compounds [29].

3.4. Effect of the Maleic Acid (MA) Dosage on the Swelling Capacity of SAH Superabsorbent Hydrogel

Figure 5 below is a graph obtained after the determination of the effect of maleic acid (crosslinker) dosage during the synthesis of superabsorbent hydrogel. 5 samples were prepared in triplicate with varied amounts of MA in the range of 1, 2, 3, 4, and 5 M of 5 mL, and the mean percentage swelling was obtained when 2 g of each of the triplicate hydrogel samples were immersed in deionized water for 24 hours.

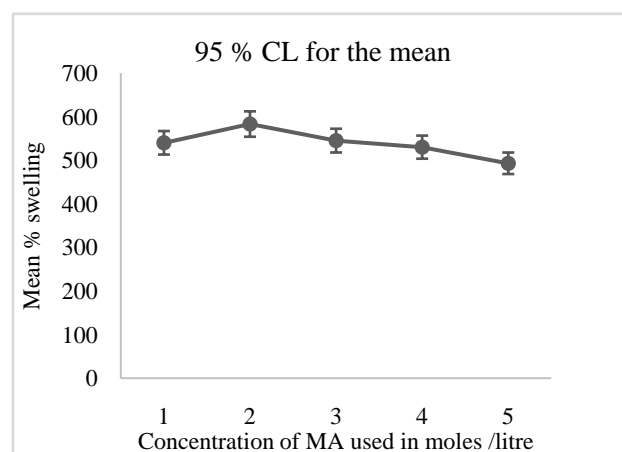


Figure 5. The effect of MA (crosslinker) dosage to the swelling capacity of the SAH (10 g AH, 4 mL GL and 5 mL of 2.0 M NaOH)

Figure 5 showed that there was a significant increase ($p < 0.05$) in the swelling percentage from 540% to 583% when the dosage of MA was increased from 1.0 M to 2.0 M, followed by a significant decrease ($p < 0.05$) to 493%. The increase was attributed to increased hydrophilic functional groups caused by overhanging modifications on the backbone of AH, which enhanced absorption of water [30], while the decrease as the dosages of MA increased above 1.0 M in 5.0 mL was ascribed to an increased degree of crosslinking. Over crosslinking increases hydrogel density, making the hydrogel tough and rigid, resulting in decreased spaces available for water absorption into the network structure [31]. Therefore, the optimum amount of maleic acid crosslinker to prepare superabsorbent hydrogel SAH was 2.0 M in 5 mL.

3.5. Effect of the Amount Glycerol (GL) on the Swelling Capacity of the Superabsorbent Hydrogel SAH

The effect of the GL concentration was determined by preparing samples of hydrogel in triplicate while varying the amount in the dosages of 2, 4, 6, 8, and 10 mL, respectively. Figure 6 show the mean percentage swelling when 2 g of each triplicate synthesised SAH sample was immersed in distilled water for 24 hours.

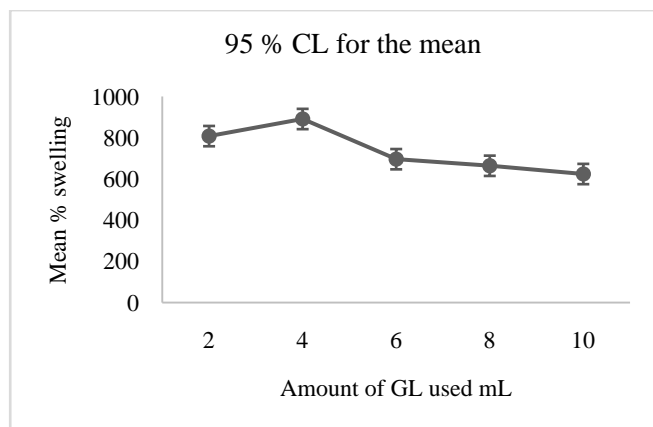


Figure 6. The effect of GL dosage on the swelling percentage of superabsorbent hydrogel SAH (10 g AH, 5 mL 2.0 M of (MA) and 5 mL of 2.0 M NaOH)

Figure 6 showed there was a significant increase ($p < 0.05$) in the swelling percentage of the hydrogel from 808% to 891% as the dosages of GL increased from 2 mL to 4 mL, followed by a significant decrease ($p < 0.05$) as the dosage was increased from 4 mL to 10 mL. The increase was attributed to the increased crosslinking density as the GL chains increased, leading to increased chain entanglement and curling degree, which elevated the carboxyl and hydroxyl hydrophilic groups per unit [32]. The decreased percentage of swelling was attributed to the excess amount of GL over AH, which led to an imbalance between carboxylate and hydroxyl functional groups of the monomers [33]. The optimum amount of glycerol required to synthesize SAH was 4 mL. Therefore, the mass ratio of AH: GL: MA (10:4:1) was used to prepare SAH gel with optimum swelling capacity.

3.6. Effect of Contact Time on the Percentage Swelling of the Superabsorbent Hydrogel SAH

The contact time was investigated by immersing 24 portions of 2 g of SAH samples in triplicate in distilled water and determining their swelling capacity at time intervals of 0.5, 1, 2, 4, 6, 8, 12 and 24 hours. Figure 7 below shows the graph obtained on the mean swelling percentage as a function of time in hours for the superabsorbent hydrogel.

Figure 7 showed that there was a significant increase ($p < 0.05$) in the swelling percentage capacity as contact time increased from 0.5 to 6 hours attaining a maximum swelling capacity of 905% and no significant increase ($p > 0.05$) as the contact time increased from 6 to 24 hours. The steady increase in the swelling percentage in the first 6 hours was attributed to a higher water affinity due to an increased number of hydrophilic functional groups on the surface of the hydrogel, coupled with the ability of hydrogen bond formation between water and hydrogel [10]. The decreased rate of absorption after 6 hours can be attributed to the saturation of the hydrogel network causing a depreciation on the gradient of water as well as a reduction of electrostatic repulsion due to decreased hydrophilic groups [34].

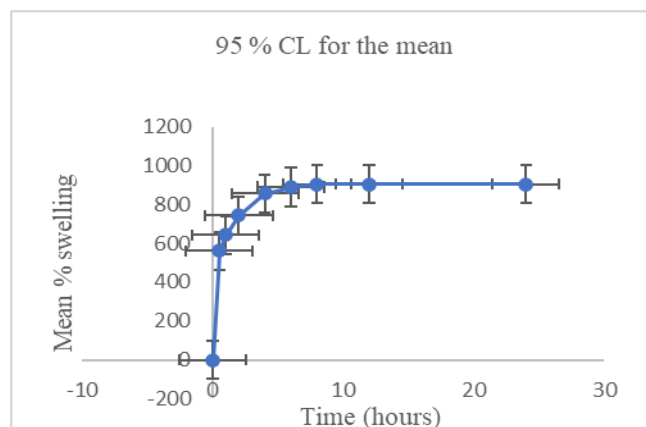


Figure 7. The effect of the contact time of 2 g superabsorbent hydrogel SAH

4. Conclusions

The findings of this study showed that the superabsorbent hydrogel (SAH) mass ratios of AH:GL:MA as 10:5:1, synthesized, gave the maximum swelling capacity. The FT-IR technique demonstrated a spectral peak at 1711.85 cm^{-1} that was ascribed to COO^- for ester linkage upon crosslinking. SEM analysis showed dense porous surface networks of SAH compared to rigid surfaces of uncross-linked polymer units (AHGL) with fewer and unevenly distributed pores. The XRD technique showed that hydrochar and AH had an amorphous nature, while polymer units (AHGL) and SAH showed semi-crystalline and crystalline structures, respectively. When 2 g of hydrogel was immersed in water, a maximum swelling capacity of 905% was attained after a contact time of 8 hours. These results indicated that SAH has a potential application in agriculture in arid and semi-arid regions to increase water and mineral retainability.

DECLARATION

The authors declare that they have no known competing financial interests or personal relationships that could appear to have influenced the work described in this paper.

ACKNOWLEDGEMENTS

The authors express gratitude to Kenyatta University's Chemistry Department, Department of Physical Science Machakos University and Department of Science Technology and Engineering Kibabii University for the assistance offered during the research period.

REFERENCES

- [1] Nilimankadas, (2013). Preparation Methods and Properties

- of Hydrogel: A Review. *International Journal of Pharmacy and Pharmaceutical Sciences*, 5: 112- 117.
- [2] Reyaz A., Mushtaq A., Aabid H. (2022). An insight into synthetic and physiological aspects of superabsorbent hydrogels based on carbohydrate type polymers for various applications: A review, *Carbohydrate Polymer Technologies and Applications*, Volume 3.
 - [3] Lee, J., Cuddihy, M., and Kotov N. (2008). Three-dimensional cell culture matrices: state of the art. *Tissue Engineering Part B*. 14(1): 61–86.
 - [4] Chang, C., Duan, B., Cai, J, and Zhang, L. (2010). Superabsorbent hydrogels based on cellulose for smart swelling and controllable delivery. *European Polymer Journal*, 21: 92–100.
 - [5] Zhu, J. (2010). Bio-active modification of poly (ethylene glycol) hydrogels for tissue engineering. *Biomaterials journal*, 31(17): 4639–4656.
 - [6] Tan, H., and Marra, K. (2010). Injectable, biodegradable hydrogels for tissue engineering applications. *Materials journal*, 3: 1746–1767.
 - [7] Anah, Lik., and Astrini, N. (2015). Hydrogel Super Absorbent Polymer (SAP) Crosslinking Agent Water-Soluble Carbodiimide (WSC). *Journal cellulose*, 5 (1): 1–6.
 - [8] Isahak, N.R. (2013). Highly porous carbon materials from Biomass by Chemical and Carbonization method; A Comparison study. *Journal of Chemistry*, 2013: 1-6.
 - [9] Yahya, A., Mansor, H., Zolkarnaini, W., Aminuddin, A., Mohamad, K., and Ozair, N. (2018). A brief review on activated carbon derived from agriculture by-product. *AIP Conference Proceedings*. 030023: 1-8.
 - [10] Titus, M., Harun, M., and Francis, M. (2022). Super Absorbent Hydrogel Derived from Activated biochar Functionalized with Ethylenediamine and Cross-linked with Maleic Acid. *International Journal of Materials and Chemistry*, 12(1): 1-9.
 - [11] Khodami, S., Kaniewska, K., Karbarz, M., and Stojek, Z. (2023). Antioxidant ability and increased mechanical stability of hydrogel nanocomposites based on N-isopropylacrylamide crosslinked with Laponite and modified with polydopamine. *European Polymer Journal*, 187: 111876.
 - [12] Bao, Y., Ma, J., and Li, N. (2011). Synthesis and swelling behaviours of sodium carboxymethyl cellulose-g-poly (AA-co-AM-co-AMPS)/MMT superabsorbent hydrogel. *Carbohydrate Polymers*, 84(1): 76-82.
 - [13] Kulkarni, V., Mutalik, S., Mangond, S, and Nayak, Y. (2012). Novel interpenetrated polymer network microbeads of natural polysaccharides for modified release of water-soluble drug: In vitro and in vivo evaluation. *Journal Pharmaceutical. Pharmacology*, 64(4): 530-40.
 - [14] Damitri, F., Bachra, Y., and Berrada, M. (2022). Synthesis and Characterization of 4-Formylphenylboronic Acid Cross-Linked Chitosan Hydrogel with Dual Action: Glucose-Sensitivity and Controlled Insulin Release. *Chinese Journal Analytical Chemistry*. 50: 100092.
 - [15] Khan, S., and Ranjha, M. (2014). Effect of degree of cross-linking on swelling and on drug release of low viscous chitosan/poly (vinyl alcohol) hydrogels. *Polymer Bull journal*. 71: 2133–58.
 - [16] Prasannamedha, G., Kumar, S., Mehala, R., Sharumitha, J., and Surendhar, D. (2021). Enhanced adsorptive removal of sulfamethoxazole from water using biochar derived from hydrothermal carbonization of sugarcane bagasse. *Journal Hazard Materials*, 407: 124825.
 - [17] Cheng, Y., Li, J., Xu, K., Huang, T., Sun, N., and Wu, Q. (2017). Effect of thermal treatment on functional groups and degree of cellulose crystallinity of Eucalyptus wood (*Eucalyptus grandis* × *Eucalyptus urophylla*). *Forest Products Journal*, 2: 135-140.
 - [18] Isaac, A., De Paula, J., Viana, M., Henriques, B., Malachias, A., and Montoro, A. (2018). From nano- to micro-meter scale: The role of microwave-assisted acid and alkali pre-treatments in the sugarcane biomass structure. *Biotechnological Biofuels*. 11: 73.
 - [19] Moe Thu, Kashio, S., Ishikawa, M, and Yokoyama, S. (2010). Effect of supplementation of dietary bamboo biochar on growth performance and body composition of juvenile Japanese flounder *paralichthys olivaceus*. *Journal of the World Aquaculture Society*, 41: 255- 262.
 - [20] Blanco. C., Martínez, A., and Tascon, D. (2000). Microporous Texture of activated carbon fibers prepared from Nomex aramid fibers. *Micropore Mesopore Materials*, 34: 171-179.
 - [21] Smith, C. (2018). *Spectroscopy* 33(7): 20–23.
 - [22] Nagaraj, P., Sasidharan, A., David, V., and Sambandam, A. (2017). Effect of cross-linking on the performances of starch-based biopolymer as gel electrolyte for dye-sensitized solar cell applications. *Polymer journal*, 9(12): 667.
 - [23] Demitri, C., Del Sole, R., Scalera, F., Sannino, A., Vasapollo, G., Maffezzoli, A., Ambrosio, L., Nicolais, L. (2008). Novel superabsorbent cellulose-based hydrogels crosslinked with citric acid. *Journal of Applied Polymer Science*, 110(4): 2453–2460.
 - [24] Somanathan, T., Prasad, K., Ostrikov, K., Saravanan A., and Krishna, M. (2015). Graphene Oxide Synthesis from Agro-aste. *Nanomaterials*. 5: 826–834.
 - [25] Hanum, F., Bani, O., and Wirani, I. (2017). Characterization of activated carbon from rice husk by HCl activation and its application for lead (Pb) removal in car battery wastewater. *Materials Science and Engineering*, IOP Conference Series: 180: 012151.
 - [26] Pradhan S. (2011). Production and Characterization of Activated Carbon Produced from A Suitable Industrial Sludge. *A Project Report*, NIT Rourkela.
 - [27] Yang, P, Xu., W., Ma, L., and Wang, Y. (2008). Characterization and acetylation behaviour of Bamboo Pulp. *Journal of Wood Science and Technology* 42: 621- 632.
 - [28] Mohamood, N., Zainuddin, N., Ahmad, M., and Tan, S. (2018). Preparation, optimization and swelling study of carboxymethyl sago starch (CMSS)–acid hydrogel. *Chemical Central Journal*, 12: 133.
 - [29] Mudgil, D., Barak, S., and Khatkar, S. (2012). X-Ray Diffraction, IR Spectroscopy and Thermal Characterization of Partially Hydrolysed Guar Gum. *International Journal Biological. Macromolecular*, 50: 1035– 1039.
 - [30] Ruhr, D., John, M., and Reiche, A. (2021). Determination of the Effective Degree of Cross-Linking of Porous Cellulose

- Membranes Cross-Linked with Bifunctional Epoxides. *Carbohydrates. Polymer*. 251: 117043.
- [31] Tanaka, F. (2011). Applications to Molecular Association and Thermoreversible Gelation. Jepang. *Polymer Physics*, Kyoto University.
- [32] Kim, J., Zhang, G., Shi, M., and Suo, Z. (2021). Fracture, Fatigue, and Friction of Polymers in Which Entanglements Greatly Outnumber Cross-Links. *Science journal*, 374: 212–216.
- [33] Mishra, A, and Malhotra, V. (2009) (2018). Tamarind xyloglucan. *Indian Journal of Pharmaceutical Sciences* 667; polysaccharide with versatile application potential. *Journal for Material Chemistry*, 19(45): 8528.
- [34] Rimdusit, K., Somsaeng, P., Kewsuwan, C., and Jubsilp, S. (2012). Comparison of gamma radiation crosslinking and chemical cross-linking on properties of methylcellulose hydrogel. *Engineering Journal*, 6(4): 15–28.

Copyright © 2025 The Author(s). Published by Scientific & Academic Publishing

This work is licensed under the Creative Commons Attribution International License (CC BY). <http://creativecommons.org/licenses/by/4.0/>